

1 2 MAR 1948

# NATIONAL ADVISORY COMMITTEE FOR AERONAUTICS

## TECHNICAL MEMORANDUM

No. 1175

FUNDAMENTAL AERODYNAMIC INVESTIGATIONS FOR DEVELOPMENT  
OF ARROW-STABILIZED PROJECTILES

By Hermann Kurzweg

TRANSLATION

“Die grundsätzlichen aerodynamischen Untersuchungen  
zur Entwicklung pfeilstabiler Geschosse”  
Schriften der Deutschen Akademie der Luftfahrtforschung,  
Nr. 1059/43, 1943, pp. 33-71



Washington  
December 1947

10 MAY 1948  
LACALBERT  
10 13 1948



NATIONAL ADVISORY COMMITTEE FOR AERONAUTICS

TECHNICAL MEMORANDUM NO. 1175

FUNDAMENTAL AERODYNAMIC INVESTIGATIONS FOR DEVELOPMENT  
OF ARROW-STABILIZED PROJECTILES\*

By Hermann Kurzweg<sup>1</sup>

I. STATE OF DEVELOPMENT OF ARROW-  
STABILIZED PROJECTILES

The numerous patent applications on arrow-stabilized projectiles indicate that the idea of projectiles without spin is not new, but has appeared in various proposals throughout the last decades. As far as projectiles for subsonic speeds are concerned, suitable shapes have been developed for some time, for example, numerous grenades. Most of the patent applications, though, are not practicable particularly for projectiles with supersonic speed. This is because the inventor usually does not have any knowledge of aerodynamic flow around the projectile nor any particular understanding of the practical solution.

The lack of wind tunnels for the development of projectiles made it necessary to use firing tests for development. These are obviously extremely tedious or expensive and lead almost always to failures. The often expressed opinion that arrow-stabilized projectiles cannot fly supersonically can be traced to this condition.

That this is not the case has been shown for the first time by Röchling on long projectiles with foldable fins. Since no aerodynamic investigations were made for the development of these projectiles, only tedious series of firing tests with systematic variation of the fins could lead to satisfactory results. These particular

---

\*"Die grundsätzlichen aerodynamischen Untersuchungen zur Entwicklung pfeilstabiler Geschosse." Schriften der Deutschen Akademie der Luftfahrtforschung, Nr. 1059/43, 1943, pp. 33-71.

<sup>1</sup>Due to indisposition of the author, the lecture was given by Mr. Erdmann, Peenemünde.

projectiles though have a disadvantage which lies in the nature of foldable fins. They occasionally do not open uniformly in flight, thus causing unsymmetry in flow and greater scatter. The junctions of fins and body are very bad aerodynamically and increase the drag. It must be possible to develop high-performance arrow-stabilized projectiles based on the aerodynamic research conducted during the last few years at Peenemünde and new construction ideas. Thus the final shape, ready for operational use, could be developed in the wind tunnel without loss of expensive time in firing tests.

The principle of arrow-stabilized performance has been applied to a large number of calibers which were stabilized by various means. Most promising was the development of a subcaliber wing-stabilized projectile with driving disc (Treibspiegel) where rigid control surfaces extend beyond the caliber of the projectile into the free stream. The stabilization of full-caliber, wing-stabilized projectiles with fins within the caliber is considerably more difficult. A completely satisfactory solution for the latter has not been found yet.

## II. THE PURPOSE AND NECESSITY OF AERODYNAMIC INVESTIGATIONS

The following fundamental aerodynamic investigations on flow conditions around bodies of short and long projectiles as well as their fins has been presented briefly by the author at the projectile meeting at Peenemünde on Oct. 9 and 10, 1941. These have been extended considerably by tests on pressure distributions and stability. The flow around a projectile body, 8 calibers long, with and without fins, was investigated first. After completion of these investigations and understanding of the aerodynamic relations, the structural design of projectiles which were ready for firing was started. It became obvious in the beginning that the final shape of a projectile could be obtained only through the closest cooperation between aerodynamists and designers, whose respective requirements necessitated constant compromises.

The following questions had to be answered by aerodynamic research:

1. Why does every normal nonspinning projectile tumble, which means that its aerodynamic force acts ahead of the center of gravity?

2. What is the fundamental effect of the fins?

The fact that a body can fly stable only when its aerodynamic force acts behind its center of gravity has been recognized in the meantime and will not be discussed further.

The answer to question (1) leads to the determination of force distribution over the entire surface of the projectiles. In addition to determining the resultant air force in magnitude and direction and its intersection with the axis of the projectile it was necessary to find how it originated. This also gives the answer to the second question and thus the means that must be taken to change the air-force distribution on the projectile such that the resulting air force intersects the axis behind the center of gravity.

Firing tests cannot answer these questions since they give only the drag of the projectile and tell whether it tumbles or not. Wind-tunnel tests determine the point of application of the air force from three component measurements and give exact knowledge of the air-force distribution over the body and fins from pressure-distribution measurements.

### III. CONCLUSIONS BASED ON WIND-TUNNEL TESTS

Basically a projectile can be stabilized by a drag force (force in direction of flow) as well as by a normal force (force perpendicular to the axis of the projectile). Drag forces are not desirable for a projectile since they result in a decrease in range and considerable reduction in velocity. Normal forces have no immediate effect on either one. Due to their irregular distribution along the axis of the projectile they cause the major portion of rotation of the projectile around its center of gravity.

Stabilization of a projectile by means of a drag force is shown in figure 1. A drag body is placed at a given distance behind the base of the projectile. If the projectile is at a given angle of attack, the drag body experiences certain forces which, acting through arm  $H$ , tend to return the projectile into the direction of flight. This stabilizing moment must obviously be larger than the unstable moment acting on the projectile. It is obvious that this required either an extremely large drag or one acting far behind the center of gravity. Calculations have shown that stabilization can be attained by spheres with a diameter equal to the caliber of the projectile and at the same distance from the base of the projectile as the distance between base and center of gravity of the projectile. This shows that this stabilization causes an extremely high drag (drag coefficient of the sphere  $c_w = 1$  subsonically). Furthermore, design complications arise which make this kind of solution not desirable. Figure 2 shows a long projectile which is also stabilized by drag forces. The model, suspended at its point of rotation in the wind tunnel, shows that the drag force caused by grooves in the rear portion is much too small to result in a satisfactory stabilization. Since the moments caused by drag forces are unsatisfactory one must resort to moments caused by normal forces.

The magnitude of the normal force at each point of the surface of the projectile is given by pressure-distribution tests. The model of the projectile has as many pressure orifices as possible which are connected to mercury manometers, permitting pressure readings immediately. The measured pressures, multiplied by the surface elements, give air-force components perpendicular to the surface, whose components normal to the axis of the projectile give the required normal forces.

One gets a better concept of the force distribution by cutting the projectile, perpendicular to its axis, into discs. Each of these discs has a surface ring upon which air-force elements act. This surface is usually at an angle to the axis except for the cylindrical portion. With the body at  $0^\circ$ , flow parallel to the axis, the pressure on each ring is uniformly distributed and therefore all normal forces are perpendicular to the axis. No resultant shear can therefore exist in any direction in the plane of the ring. Hence, there can

be no moment about the center of gravity. The projectile is therefore in equilibrium, which can be either stable or unstable. This question will be decided by investigating the projectile for various angles of attack.

If the projectile has an angle of attack of about  $8^\circ$ , the distribution of pressures on each ring as well as on both sides of the control surfaces is no longer symmetrical. Air-force distributions result as shown in figures 5 and 6. Resolving the individual normal-force elements into the plane of relative wind and axis of projectile, one sees that a shear force exists which is either a pressure or a suction, depending upon its sign. These forces on each ring and fin cause right- or left-handed moments about the center of gravity. One or the other can dominate along the projectile and the projectile can thus return to zero position or depart from it. Figure 3 shows the individual shear forces along the axis of the projectile with and without fins. The projectile had an angle of attack of  $8^\circ$  and was tested in the wind tunnel at subsonic speeds. The direction of flow in the figure is from the left lower corner to the upper right. Figure 4 shows a more slender projectile without fins at subsonic speed. The shear force in kilograms are referred to 1 centimeter of the axis. They were calculated for a wind velocity of 200 meters per second. (447.3 mph) and sea-level air density.

Projectiles without fins show a positive, sinusoidal shear force distribution over the ogival tip (positive upward in the figures). The cylindrical part has almost zero shear and the ogival tail has negative shear. Thus there are right-handed moments ahead of the center of gravity as well as behind which tend to turn the projectile away from the zero position. This causes an increase in force on the tip and tail with increase in angle of attack and the projectile will soon turn crosswise.

How can this be avoided? The destabilizing moments must partly be changed in sign. This cannot be done between the tip and center of gravity of the projectile since no aerodynamic means are available. It is possible though to change the moments behind the center of gravity.

The trick is to introduce surfaces parallel to the axis and having the same angle of attack as the axis at the point of the maximum right-handed moment (at 90 cm in fig. 3). This results in an air-force distribution which gives the desired moments. Behind the leading edge of the so-called shoulder of finned projectile there are extremely high suction which by far exceed the pressure forces on the side exposed to the wind. Particularly for subsonic speeds there is a high suction gradient immediately behind the shoulder which decreases rapidly towards the trailing edge of the fin. In the supersonic range the suction area is more uniformly distributed over the surface, which will be discussed in detail later. Such control surfaces have the following effects:

1. The right-handed moments of the tail of the projectiles are counteracted.
2. New left-handed (stabilizing) moments behind the center of gravity are caused which are stronger than those ahead of the center of gravity and thus tend to return the projectile to zero position.

The projectile of figure 4 shows a different shear distribution over its slender tail portion. There is no pronounced minimum. Zero shear occurs far back on the projectile and the start of the fin can also be far back which is very advantageous from previous observations. In this case small areas with little drag are sufficient. Figures 5 and 6 show the pressure distribution on cross sections of the projectile of figure 3. They are given for two supersonic velocities for the portion behind the center of gravity. Ring i contains no control surface while rings k to p show pressures over the body as well as the control surface. At q and r the control surface extends beyond the base of the projectile. Shaded areas represent pressures higher than those in undisturbed flow while unshaded areas represent pressures lower than undisturbed pressures. Fig. 5 shows that at Mach number = 1.87 the suction on the leeward side far exceeds pressures on the windward side. Furthermore, there are extremely high suction on the edge of the fin which is even more pronounced for subsonic velocities. For Mach number = 3.2 (fig. 6), the pressure conditions are changed such that the pressures on the windward side increase considerably so that the negative

pressures no longer predominate. Furthermore, the control-surface rings  $n$  to  $r$  have a more uniform pressure distribution over the entire width of the ring so that the effectiveness of the fin extends over the entire width of the fin while at lower velocities only the outer portions of the fin are effective.

Figures 7 and 8 show the normal-force distribution over the longitudinal axis of the same body for various angles of attack at subsonic and supersonic speeds. These figures give nondimensional shear-force coefficients. For subsonic speeds there is very little variation with Mach number. For supersonic speeds, though, the shear-force coefficient varies considerably with Mach number, particularly in the region of the fin.

There is a pronounced force concentration at the shoulder of the fin at subsonic speeds while for supersonic speeds there is a uniform distribution of normal force over the entire length of the fin which increases with Mach number.

Figures 7 and 8 show the variation of normal force with angle of attack of the body. The pressure and suction peaks of body and fin reduce when returning the projectile to  $\alpha = 0^\circ$ . They reduce to zero when  $\alpha = 0^\circ$ . The forces over the ogival tip do not reduce at the same rate as those over the fins. Figures 9 and 10 show two cases of completely and incompletely stable projectiles at  $\alpha = 0^\circ$ . The increase of moments ahead of the center of gravity (ogival tip) and behind the center of gravity (fin) is plotted in two curves against the angle of attack. Figure 9 shows the desired case where the left-handed fin moments are always greater than the right-handed tip moments. Thus the projectile is rotated until both vanish for  $\alpha = 0^\circ$ . Figure 10 shows that the left-handed fin moments are larger than the tip moments only for angles of attack greater than  $5^\circ$ . For smaller angles the reverse is true. This means that the projectile with this fin is unstable for small angles up to  $\pm 5^\circ$ .

From these investigations it is possible to determine the most effective position of the fins for every basic projectile body whose pressure distribution is known. It can be seen that the fin of the projectile of figure 3 should not be carried forward too far since its shoulder, with its high suction force, would approach the center of



gravity too closely, resulting in small moments. It would be absolutely incorrect to attach the fin shoulder ahead of  $L = 50$  centimeters since this region is ahead of the center of gravity and cannot afford to receive additional right-handed moments. It would be extremely unsatisfactory to extend the fins up to the tip of the projectile since they would require greater width in the rear portion to counteract the additional adverse moments at the tip. Also unsatisfactory would be a position of the fin too far back at the tail since this would counteract only part of the right-handed body moments. The latter case, though, produces large moments of the fin forces due to their large distance from the center of gravity. Hence, each case must be decided upon separately: If the counteraction of the right-handed moments by fins further forward is more effective than the large left-handed moments of fins far behind, in presence of the unstable body moments. For the projectile of figure 4, a fin, starting near the center of gravity, would be wrong since there are already considerable stabilizing moments.

After understanding the fundamental effects of control surfaces it can be seen why it is difficult to stabilize full caliber projectiles with fins not extending beyond the caliber. The fins are within the width of the projectile which means, they are exposed to air which has been accelerated by boundary layer and base vortices and thus has less impact force than the undisturbed air in the atmosphere. The tip moment of the projectile would therefore predominate, particularly for small angles of attack.

For fins within the caliber to be effective one must take care that the flow will nowhere separate from the body of the projectile so that the nonseparated flow adheres everywhere to the projectile. The fins are then exposed to this nonseparated relatively undisturbed flow. It is particularly difficult to taper the projectile towards the rear so that the flow at angles of attack does not separate. In most cases there will be separation for a certain velocity range, figure 11. Even for nonseparated flow the boundary layer increases beyond the maximum diameter of the projectile so that the fins are no longer in an undisturbed flow. Hence, fin stabilization (at least for one point,  $\alpha = 0^\circ$ ) is basically insufficient with normal forces of full-caliber projectiles. Drag forces must therefore be employed for stabilization.

## IV. THE BASIC BODY

Few general statements can be made concerning the shape of the basic body (projectile without fins). The design of the projectile depends on its ultimate purpose, namely, to obtain large ranges with small mass, to carry large masses over small ranges, as subcaliber driving disc projectile, as full-caliber projectile, and so forth. Out of the large number of projectile tests only one particular investigation is shown and the results discussed. It was attempted to find the optimum shape for the drag of the basic body of a driving disc projectile of given mass with a given base area which could not be reduced for reasons of strength. Starting with a basic body 0, figures 12 to 15 show four body families having certain equal characteristics. These have been varied in a certain manner and the respective drag at  $\alpha = 0^\circ$  and  $Ma = 2.5$  measured.<sup>2</sup>

Body families a and b (figs. 12 and 13) have as characteristics, equal length and variable volume. Body family a has furthermore the same tip angle of  $32.5^\circ$  while family b varies the tip angle from  $23^\circ$  (body 1) to  $44^\circ$  (body 9). The maximum cross section for body family b occurs approximately at the same distance from the base while it moves rearward in the case of body family a due to the tip angles being equal. Body families c and d, (figs. 14 and 15), have as common characteristics, equal volume and variable length. Family d has again equal tip angles and family c increases its tip angles from body 1 to 9. For both these families, body 1 did not give presentable wind-tunnel data. The three ordinates shown in the diagrams give the drag coefficients  $c_w$  referred to three areas: body surface (O), (volume)<sup>2/3</sup> ( $V^{2/3}$ ), and maximum cross section (Q). Depending on the point of view and purpose of comparison one can use any one of these reference areas. Body family a shows relatively constant  $c_w(V^{2/3})$  and  $c_w(O)$ .  $c_w(Q)$  decreases due to the large increase in maximum cross section. Body families b and c show large increases of  $c_w(V^{2/3})$  with tip angle. For body family c one sees that the friction drag  $c_w(O)$  for the very long body number 2 approaches

---

<sup>2</sup>All bodies bearing the same number have the same maximum cross-section.

almost that of a flat plate in subsonic flow. Hence, there is almost no pressure drag. For body family d,  $c_w$  behaves similarly except that it is not much higher for the fatter body since the tip angles remain the same.

The investigation of these families shows amongst other things that the tip angle has the greatest effect upon the drag of the body and that it should be kept as small as possible in all cases. Comparison of two bodies of equal volume, bodies number 9 of families c and d, show that it is better to move the maximum cross section far back to keep the tip angle small rather than to provide a slender tail as is required in the subsonic flow. This is contrary to the important requirement that the center of gravity should be as far forward as possible. It is obvious that the choice of the optimum basic body is not easy since additional requirements must be considered such as ballistic questions, explosive content, fuse shape, and structural problems.

## V. THE CONTROL SURFACES

Shape and size of control surfaces for subcaliber driving disc projectiles can be determined from wind tunnel tests on flat plates in subsonic and supersonic flow. They must produce the necessary counteracting moments. The optimum shape and size on the other hand must be determined by the above mentioned method.

As to shape, it is fundamentally required that the leading edge of the fin be very sharp to give as small as possible a profile drag. This sharp edge, which should also be used for the tip of the fin, produces also a very high suction peak on the upper surface of the surface whose low pressure around the sharp edge will not equalize with the high pressure on the lower surface. About a rounded edge there is a flow by which the suction of one side is reduced by the pressure of the other side. For the lateral edge of the fin a sharpening is usually not desired for practical reasons. This edge should then not be rounded but should be made rectangular. A sweepback angle (fin leading edge versus axis of projectile) of  $50^\circ$  has been found very practical.

Smaller angles make a fin less effective, larger ones increase the drag. It is particularly advantageous to widen the fins towards the back so that the outer edge makes an angle of approximately  $30^\circ$  with the axis of the projectile. This increases the stabilizing effect by having the rearward position of the outer edge in undisturbed flow. This inclination of the outer edge can usually not be used for driving disc projectiles because the maximum width of the fin is limited and no loss in area can be afforded. This design is particularly suited for rocket projectiles which have no limitation as to the maximum diameter.

The effectiveness of fins can furthermore be increased by providing several shoulders, figure 16. The control surface as a whole counteracts the right-handed moments behind the center of gravity of the body. Each individual shoulder builds up a suction peak. The force of the first shoulder is at the same distance from the center of gravity as that of a single shoulder fin. The forces though are slightly smaller, but the suction peaks, lying further back, being also smaller than the single shouldered ones, have a larger distance from the center of gravity and produce, therefore, larger left-handed moments. Unfortunately, this type of control surface is not suited for a driving disc projectile because of the insufficient space between projectile and caliber. This would make the width of the individual shoulders too small, thereby eliminating their effectiveness. These fins also have their place only for rocket projectiles.

Tests have been made at Peenemünde to determine the best number of fins. In principle, a four-finned control surface can produce stabilizing moments. This type of control surface though produces a slight roll in projectiles which not only occurs due to flight unsymmetries in the control surfaces but also at any angle of attack. If the projectile flies with an angle of attack, as is the case for nonlinear flight or with side wind, the cross-like four-fin arrangement causes rolling moments about the longitudinal axis. This rolling moment has a maximum for a lateral angle of the relative wind of  $\varphi = 22\frac{10}{2}^\circ$ . It is zero for  $\varphi = 0^\circ$  and for  $\varphi = 45^\circ$ . (See fig. 17.) The same condition exists for angles between  $45^\circ$  and  $90^\circ$ .

This causes rolling frequencies which may easily be in resonance with the aerodynamic natural frequency of the projectile and may thus lead to three-dimensional oscillating motions.

It is, therefore, recommended to use more than four fins which, on the other hand, causes larger drag. Practice has shown six fins to be sufficient which cause only slight rolling moments and only a slight drag increase.

## VI. THE THICKNESS OF THE BOUNDARY LAYER FOR WIND-TUNNEL MODEL AND FULL-SCALE PROJECTILES

When applying wind-tunnel tests to the full-scale projectile at supersonic speeds it is usually sufficiently accurate if the same Mach number exists for the flow in both cases. For more exact investigations, the Reynolds' number of the flows must be considered, which is particularly important when investigating surface friction and boundary layer growth. The growth of the boundary layer along the projectile, full scale and model, can be of great importance for the fins. It has been mentioned how important it is that the fins extend into unseparated flow. A thick boundary layer makes a larger portion of the fin more ineffective than a thin one. The boundary layer grows as a certain function of the length of the body, whereby the velocity and viscosity of the surrounding air are of importance. These conditions which are determined by Reynolds' number are usually not the same for full-scale and wind-tunnel models. No experience exists of boundary-layer conditions for projectiles in supersonic flow. Certain statements can be made though when considering the boundary layer on flat plates which are sufficiently known for subsonic speeds. Considering for instance, a full-scale projectile of two-meter length and a caliber of 18 centimeters, flying with a speed of 1100 meters per second (2460 mph), the thickness of the boundary layer at the tail of the projectile is  $\delta = 1.85$  centimeters = 0.10 caliber. If the wind-tunnel model is 10 centimeters long and has a caliber of 3.6 centimeters, measured at a Mach number = 3.25, the boundary-layer thickness at the corresponding point is  $\delta = 0.80$  centimeters = 0.22 caliber.

Although this boundary-layer method is valid only for flat plates, it would give at least a qualitative insight if applied to round projectiles. This means that the model has twice as much of its fin in the boundary layer than the full-scale projectile. Hence, the stability of the projectile as measured in the wind tunnel must be on the safe side. The full-scale projectile will be even more stable.

## VII. DEFINITION OF STABILITY

When counteracting the destabilizing force distribution, known from pressure-distribution tests on the basic body, by means of a control surface or sometimes by changing the shape of the basic body, the arrow-stabilized projectile may show the following behavior in the air stream:

(a) It is stable. That means it will return to its undisturbed position out of its own account when displaced from zero position. This type of projectile is called "point stable" at Peenemünde. That means it has only one stable position which has zero moments. If this zero-moment position coincides with  $\alpha = 0^\circ$  the projectile is "arrow stable" without restriction. Figure 18 shows such a projectile whose center of gravity lies at approximately  $H/D = 6$ . The corresponding variation of the moment is shown in figure 19.

The moment arm of the air force is always positive for positive and negative angles of attack. The moment diagram shows only one zero for  $\alpha = 0^\circ$ . The tangent to the  $c_m$ -curve is positive, thus indicating stability of the projectiles.

(b) It is unstable. This means that it departs on its own account to very high angles of attack, from the zero position, when disturbed. Such a projectile turns crosswise and cannot be used. The projectile of figure 20 is such a type. The center of gravity lies at about  $H/D = 4$ . The corresponding moment distribution is shown in figure 19. The projectile is unstable, the moment arm  $p$  of the air force is always negative. So is the tangent to the moment diagram at  $\alpha = 0^\circ$ . This indicates unstable conditions at the only zero point.

(c) It is stable in one position and unstable in another. In most cases unstable conditions exist for small angles of attack which change into stable conditions for larger angles of attack. Such projectiles are called "circle stable" at Peenemünde. That means that there are three zero moment positions when oscillating in a plane whereby the position at  $\alpha = 0^\circ$  is unstable and those for angles of attack  $\pm\alpha$  are stable ones. When oscillating in space the zero moment positions have a circle as locus.

If this value of  $\alpha$  is small, such a projectile is called "partly arrow stabilized." The moment diagram is shown in figure 19. The moment arm  $p$  is negative for small angles of attack and positive from  $\pm\alpha$  on. The moment curve has three zeros. Its tangent is negative for  $\alpha = 0^\circ$ . The projectile is unstable at this point. The tangent is positive at  $\pm\alpha$  thus indicating stable conditions of the projectile. This is the most commonly experienced case of stability. Even highly developed arrow-stabilized projectiles show this property, but in most cases only for a very narrow range of angles.

(d) The opposite case of stable at small and unstable at high angles of attack occurs only occasionally. Such projectiles should be called "circle unstable." Figure 21 shows a projectile whose moment arm decreases with increasing angle of attack. Figure 19 shows the moment arm positive for small angles and negative from  $\pm\alpha$  on. The moment diagram has again three zeros. The tangent at  $\alpha = 0^\circ$  is positive thus indicating stability of the body at  $0^\circ$ . At  $\pm\alpha$  the tangent is negative thus showing unstable conditions.

#### VIII - FIRST PROPOSAL FOR AN ARROW-STABILIZED PROJECTILE BASED ON AERODYNAMICS

The investigation of air-force conditions on body and fin discussed led the author to his proposal of an arrow-stabilized projectile with sliding control surfaces. This was done to improve the Röchling projectiles and to replace their folding fins by rigid fins. If rigid fins are attached to a projectile body,

15 calibers long, on the same place as the folding fins, there was not enough space for each individual fin. Thus the fin surface would be too small. To extend them forward in order to gain more area is of no use and can be very detrimental. The only possible way to produce stabilizing moments is by moving the control surfaces backwards after the projectile has left the barrel. The correctness of this has been shown in wind-tunnel tests and firing tests.

This model (fig. 22) shows for the first time how an arrow-stabilized long projectile with fixed fins must look in flight so that all aerodynamic conditions are satisfied and that it can be fired as a driving disc projectile with the presently available discs.

The designer had thus a projectile capable of flight which had to be investigated for strength of body and fin and for simple and practical firing procedure. It was particularly required to avoid the sliding of the fin since moving parts in a projectile are not desired. One tried to move the fin far back from the beginning so that the aerodynamic conditions remained satisfied and still permitted flying. Mr. Gessner of the Aerodynamischen Institut der Heeresanstalt Peenemünde devised constructive solutions of this problem, namely the "driving cone," "driving fin," and "driving ring."

## DISCUSSION

### Mr. Haack

I would like to add a few remarks about theoretical work done at my Institute pertaining to wing-stabilized long projectiles which are based on Peenemünde projectiles.

I determined some time ago the meridian of a round body whose pressure-drag was a minimum for given caliber and volume but variable length. This was done by an approximate solution of the linearized differential equation. Figure 1<sup>3</sup> shows the projectiles with three

---

<sup>3</sup>Translator's note: The four figures referred to in the Discussion may be found at the end of the figures for the report.



such bodies of equal caliber and volume (represented by the cylinder). To obtain a minimum the length may vary between these limits. The first and longest shape represents the optimum, the other shapes result from reducing the length. The shortest form results from the condition that the projectile shall have no cylindrical center portion.

1. I have devised a new arrow projectile based on a Peenemünde projectile of the same caliber and volume but with an optimum meridian. The longest shape, having at the same time the smallest pressure drag, was impractical for reasons of stability. Figure 2 shows the Peenemünde arrow and the arrow with optimum meridian of equal volume and caliber (different scales in this figure. The control surface had six fans).

For the volume and caliber as given by the Peenemünde arrow, the length limits of an optimum projectile are between 15 and 22 calibers. This considers the body without fins with a pointed tail. The over-all length of the Peenemünde arrow is 12.25 calibers, for the optimum arrow the length was limited to 18 calibers.

2. Of particular interest is the calculation of the drag. First, the drag of the Peenemünde arrow at Mach number = 2 was calculated and was compared with wind-tunnel tests; then, the same calculation was carried out for the optimum arrow to determine the gain due to an optimum meridian.

The drag was calculated as the sum of pressure drag, friction drag, and base suction. The pressure drag was calculated from Kármán's linearized theory for slender projectiles in supersonic flow. This led to the following simplified method: the meridian of the body was replaced by a polygon of secants with end points  $x_i, r_i$  and the slopes

$$r_i' = \frac{r_i - r_{i-1}}{x_i - x_{i-1}}$$

Let  $\xi = x_1 - ar_1$  where  $a$  is the cotangent of the Mach angle. The over pressure at points  $r_n$  and  $x_n$  of the meridian is then determined by the equations

$$A_n = \frac{r_n r_{n'} - \sum_{i=1}^{n-1} A_i (\xi_i - \xi_{i-1})}{x_n - \xi_{n-1}} \quad (1)$$

$$\frac{p - p_0}{\frac{\rho_0}{2} U_0^2} = -2 \sum_{i=1}^n A_i \left( \text{Arcos} \frac{x_n - \xi_i}{ar_{i1}} - \text{Arcos} \frac{x_n - \xi_{i-1}}{ar_n} \right)$$

The pressure drag is then found by integration

$$c_{\text{wave}} = \frac{2\pi}{\frac{\rho_0}{2} Q U_0^2} \int_e r r' (p - p_0) dx; \quad Q = \text{cross section}$$

Friction drag and base suction are calculated according to the following equations

$$c_{\text{friction}} = \frac{0.362}{2\pi} \left( \frac{2v_0}{U_0 L} \right)^{0.2} \frac{\text{Surface}}{\text{Area}} : v_0 = 133 \times 10^{-7} \quad (2)$$

$$c_{\text{suction}} = 0.2 \left( 1 - 0.2 \frac{U_0^2}{4a^2} \right) \frac{Q_{\text{base}}}{Q_{\text{max}}} \quad (3)$$

where

$U_0$  velocity of projectile in meters per second  
 $v_0$  kinematic coefficient of friction  
 $L$  length of projectile in meters  
 $a$  velocity of sound in meters per second

These equations give the following drag coefficients at Mach number = 2 for the Peenemünde arrow (PPG) and the optimum projectile (Hk)

		PPG	Hk
$c_{\text{wave}}$	(Pressure drag)	0.11	0.03
$c_{\text{friction}}$	(Friction drag)	.10	.13
$c_{\text{suction}}$	(Base drag)	.13	.13
$c_{\text{total}}$		.34	.29

One sees that the pressure drag of the optimum projectile is only one-fourth of that of the PPG. The over-all gain in drag, though, is not very large. It should be mentioned here that the pressure drag of the shoulders of the fins cannot be calculated easily. Hence, the pressure drag of the entire body without fins was calculated and it was assumed that the pressure drag of the wings equals that portion of the pressure drag which acts over the surface of the body covered with wings.

As to wind-tunnel tests it should be remembered that these were made not on the original projectile but on a considerably smaller model and that therefore the friction drag coefficient will be different from a normal model. The drag of the model, one-fifth full scale, under normal air conditions, is found according

to equation (2) by multiplying this value by  $\sqrt[5]{5}$ , using values of the full-scale projectile given above. Thus for the PPG  $c_{\text{friction}} = 0.11$  and hence  $c_{\text{total}} = 0.38$ . I was told that the value as measured in the wind tunnel is  $c_{\text{measured}} = 0.39$ . This excellent agreement is beyond all expectations.

3. Finally a few remarks on the fins of the optimum projectile. For the new projectile the wings of the control surface had to be extended far forward. This is necessitated by the distribution of the shear forces which were calculated by a linearized method for small angles of attack. The shear distribution is shown in figure 3 for Mach number = 2. It is advisable to start the fins at the point where the shear forces on the tail start to increase the moment. The center of gravity is approximately 10.4 calibers from the nose. Only a test will show if this center-of-gravity position and these fins are satisfactory for stabilization.

#### Mr. Sauer

Oscillation of finned projectiles are mathematically simpler to solve than those of spinning projectiles for two reasons: First, one can limit oneself to small angles of attack, since there is no excitation, and therefore linearize the differential equation. Second, the coupling with the center-of-gravity oscillations is so small, due to the low frequency, that the oscillation of the axis of the projectile can be satisfactorily approximated by the undisturbed path of the center of gravity ( $\alpha = 0^\circ$ ) neglecting coupling.

To best describe the oscillating motion one uses a moving system of coordinates  $\xi$ ,  $\eta$ , and  $\zeta$  whose origin lies on the undisturbed path of the center of gravity and, their axes are the tangent, principle, normal, and binormal of the path. The end point of the unit vector in direction of the axis of the projectile describes the "oscillation curve" in the  $\xi$ ,  $\eta$ , and  $\zeta$  system. Its projectiles are combined in the complex angle of attack  $\alpha = \xi + i\eta$ . The oscillation curve satisfies the following equation of motion:

$$\ddot{\alpha} + 2\lambda\dot{\alpha} + \mu^2\alpha = -i(2\lambda\dot{\zeta} + \ddot{\zeta})$$

$$\text{where } \lambda = \text{const. } v_{yc_d}, \quad \mu^2 = \text{const. } v^2 \gamma c_m'$$

In this equation, the angle of inclination  $\theta$ , the velocity  $v$ , the Mach number  $M$ , and the specific weight of air  $\gamma$  are given as functions of time from the undisturbed path. The damping coefficient  $C_d(M)$  and the derivative  $c_m'(M) = dc_m/d\alpha$  of the moment coefficient follow from wind-tunnel tests.

Integration of the equation of motion leads to damped oscillations. In this manner the oscillations of a very long projectile were calculated for the instant of firing and the disturbance occurring near its maximum height. The initial or firing oscillation damps out very quickly while the apex oscillation extends over a large portion of the descending path.

The initial oscillations are replaced by an equivalent disturbance of initial conditions of the undisturbed flight path. The data investigated at Aachen resulted in disturbance values which were almost constant over a large range ( $v_0$  from 300 to 1100 meters per second (1790 to 2460 mph) and  $\theta_0$  from  $20^\circ$  to  $45^\circ$ ). It is said that the dispersion caused by oscillation is caused primarily by variation in the initial direction, while the  $v_0$  variation is negligibly small. The variation of the initial angle is of magnitude of  $1^\circ$ , the  $v_0$  reduction of magnitude of 1 meter per second.

#### Mr. Busemann

Considering projectiles with given caliber, given volume, and given length having the least resistance, one sees that this problem of minima is overdetermined since the three quantities are not entirely independent from each other. Caliber and volume determine the minimum length of the projectile, namely, the length of the cylinder made up of caliber and volume. A maximum length was determined by Mr. Haack, above which further reduction of drag is not possible when retaining the two other conditions. Between these two limiting lengths there is for each given length a well defined minimum body. If the lengths are not much larger than the length of the cylinder, the minimum body consists of a cylindrical center portion with added nose and tail tips. Only for larger lengths do nose and tail tips come together at the center of the projectile and the cylindrical center portion disappears.

This latter class has been calculated by Mr. Haack since they permit an analytical expression for the meridian over the entire length of the projectile. Missing, though, is the shape of projectiles of small lengths, made up of three parts, which is to be found from a mixed problem of minima. For the meridian of nose and tail tips, all additional conditions must be considered while the cylindrical center portion is primarily determined by the given caliber.

#### Mr. Stange

The increase of arrow projectiles depends considerably on the caliber. The quoted figure of 50-percent increase in range as compared to the spinning projectile refers to a caliber of 28 centimeters. When increasing the diameter  $D$ , conditions are considerably worse since the equation for the drag deceleration contains  $D^2$  in the numerator and the weight in the denominator which is proportional to  $D^3$  for relatively equal weights of projectiles. Hence, the drag deceleration of the projectile is proportional to  $1:D$  for otherwise equal conditions. Thus the gain in range, when changing from the spinning projectile to an arrow projectile, will become gradually less and less. Approximate calculations show that under conditions mentioned the range increase for  $D = 28$  centimeters is 50 percent, at  $D = 30$  centimeters only 10 percent at the most. Figure 4 shows the conditions for a diameter ratio  $D:D' = 100:64 \approx 5:2$  ( $D =$  spinning projectile,  $D' =$  arrow projectile).

#### Translator's Note

The rest of the discussion deals mostly with ballistic problems such as penetration, charge, materials and accuracy, and does not contain any information of interest in conjunction with the original paper.

Translated by H. P. Liepman  
Goodyear Aircraft Corporation

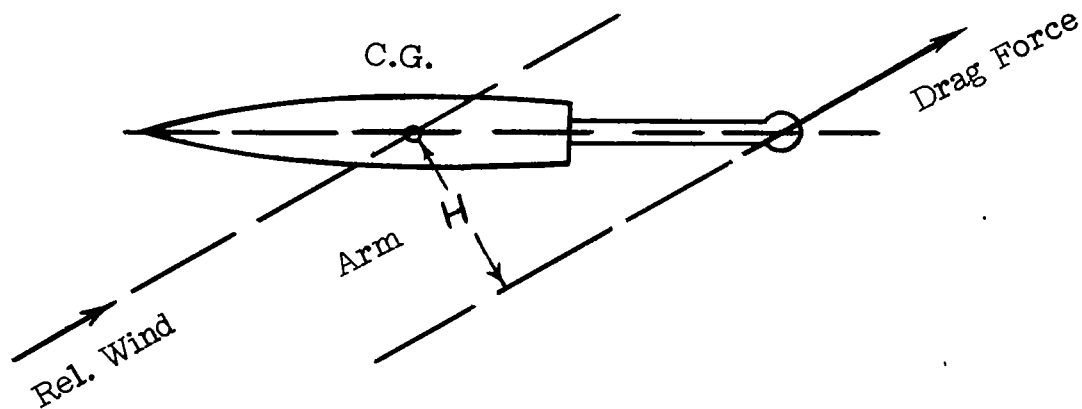


Figure 1.- Drag stabilization of a projectile.

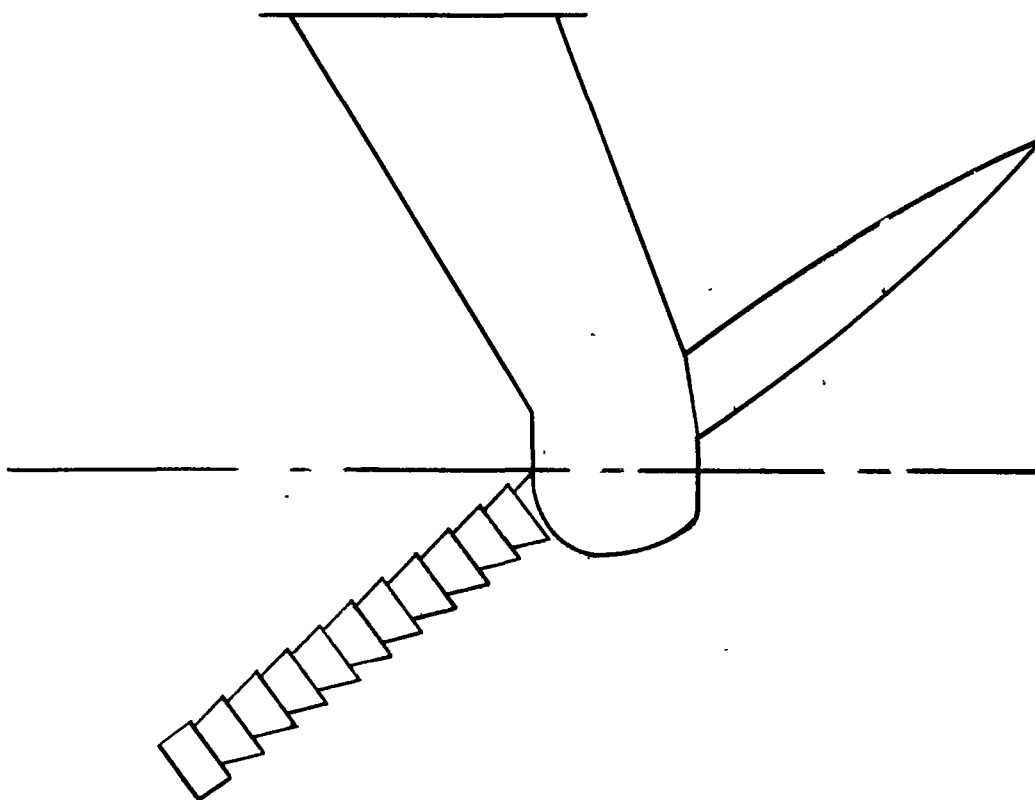


Figure 2.- Insufficient drag stabilization.

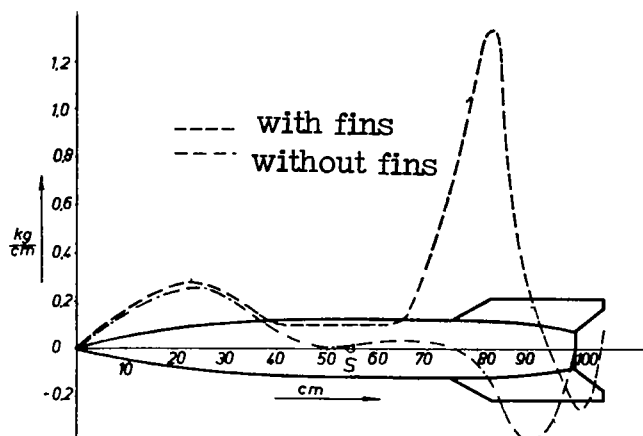


Figure 3.- Shear force distribution on a projectile with and without fins.  
 $\alpha = 8^\circ$   $v = 200$  m/s = 656 ft/sec.

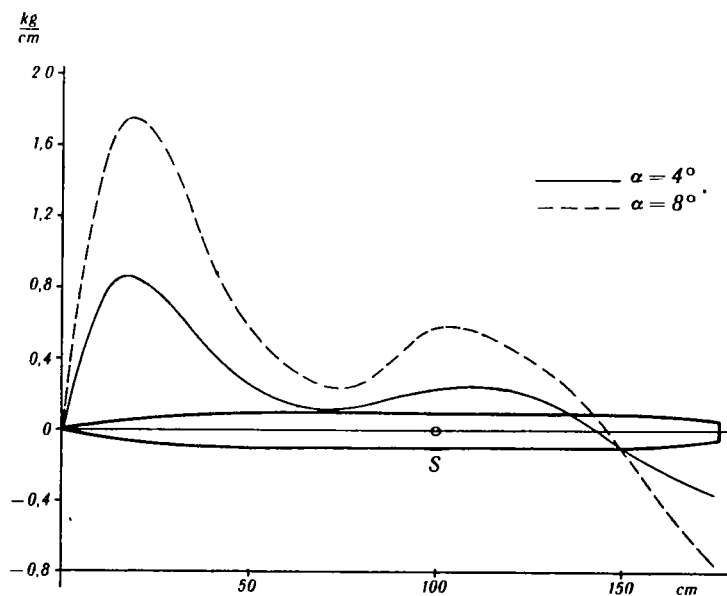


Figure 4.- Shear force distribution over an arrow projectile without fins. 17.6 calib. long.  $v = 200$  m/s.



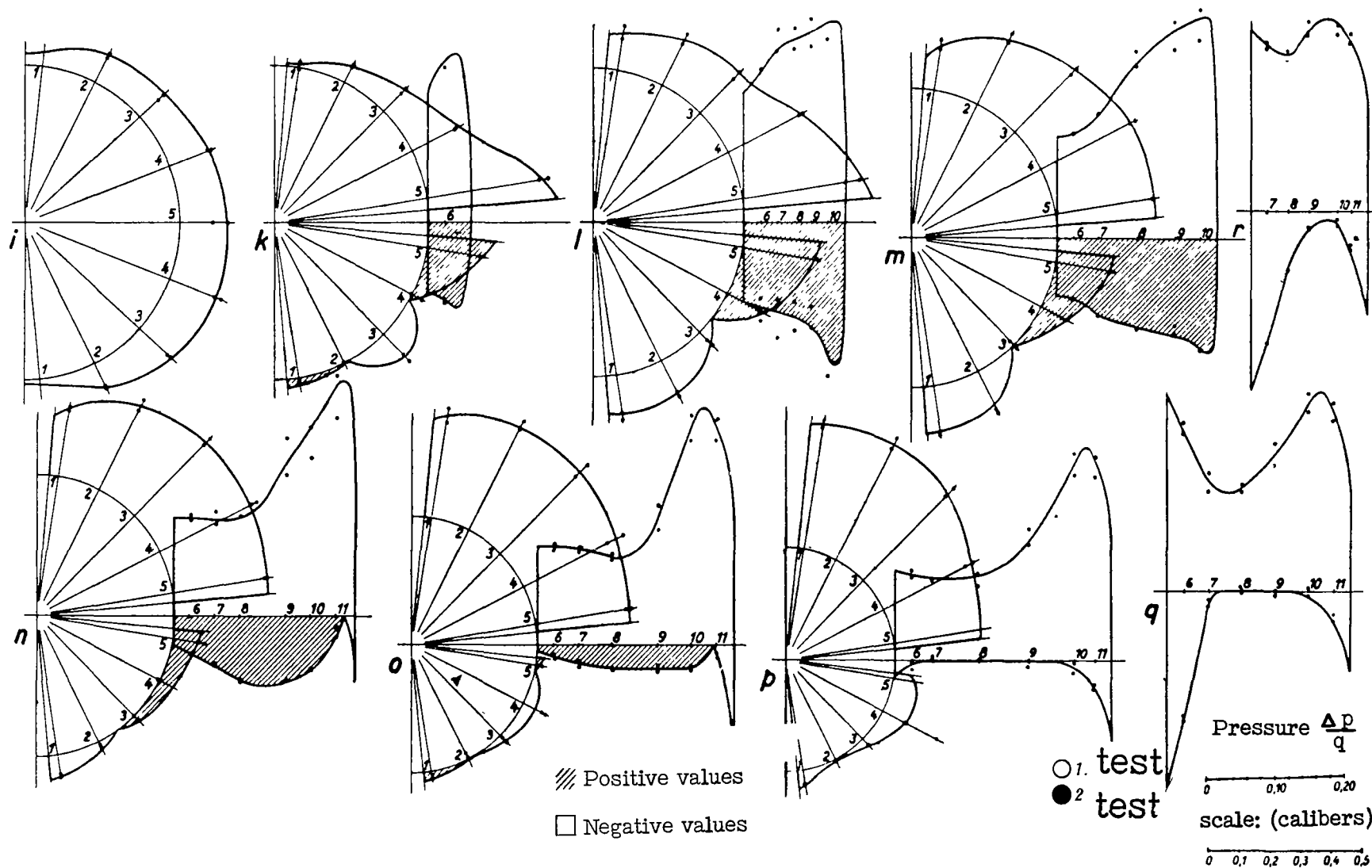


Figure 5.- Pressure distribution tests on missile A4VIP. Pressure distribution at  $M = 1.87$ , plotted perpendicular to surface ( $\alpha = 8^\circ$ ), over various tail wings and fin sections.

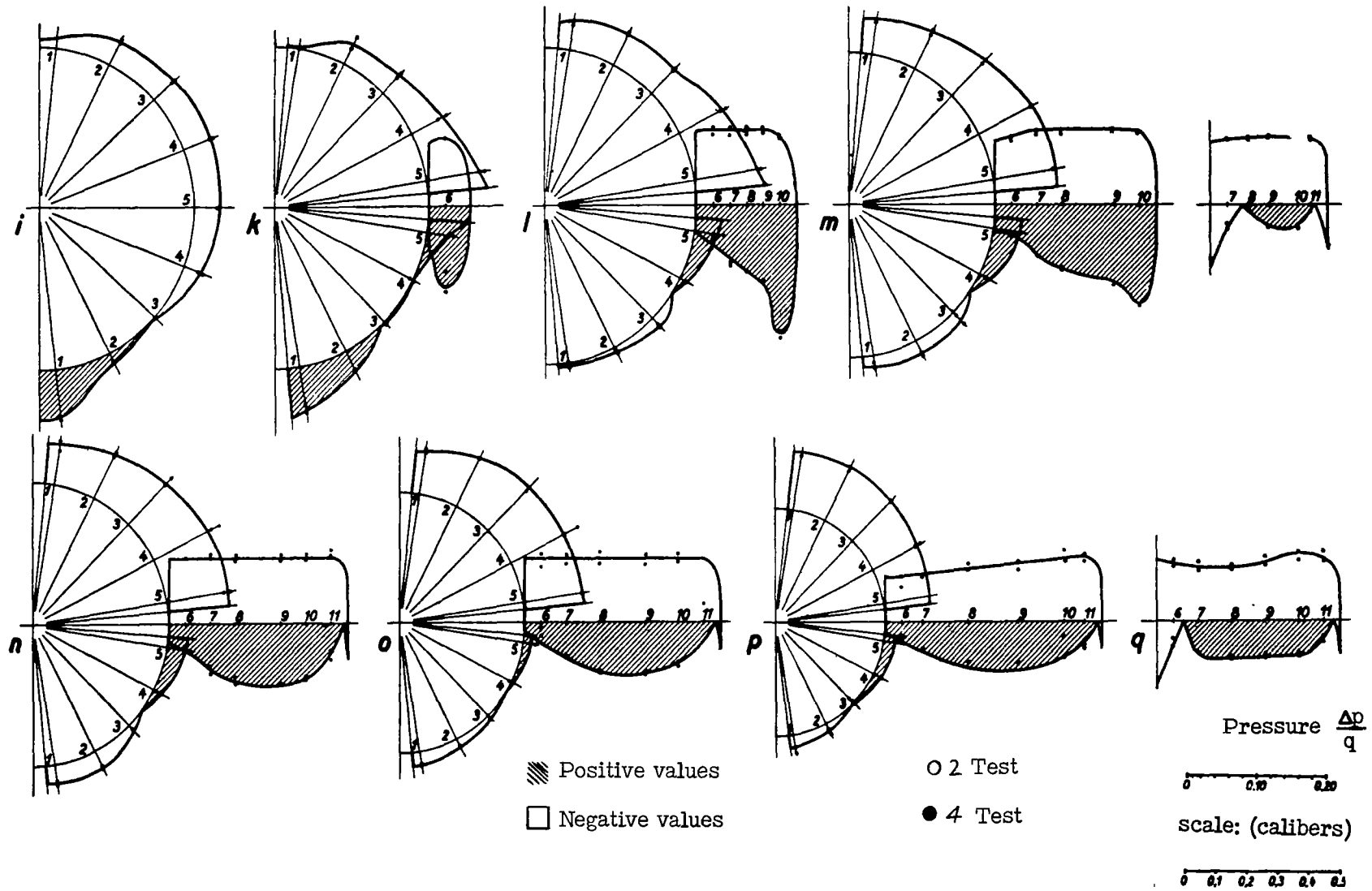


Figure 6.- Pressure distribution tests on missile A4VIP. Pressure distribution at  $M = 3.24$ , plotted perpendicular to surface ( $\alpha = 8^\circ$ ) over various tail wings and fin sections.

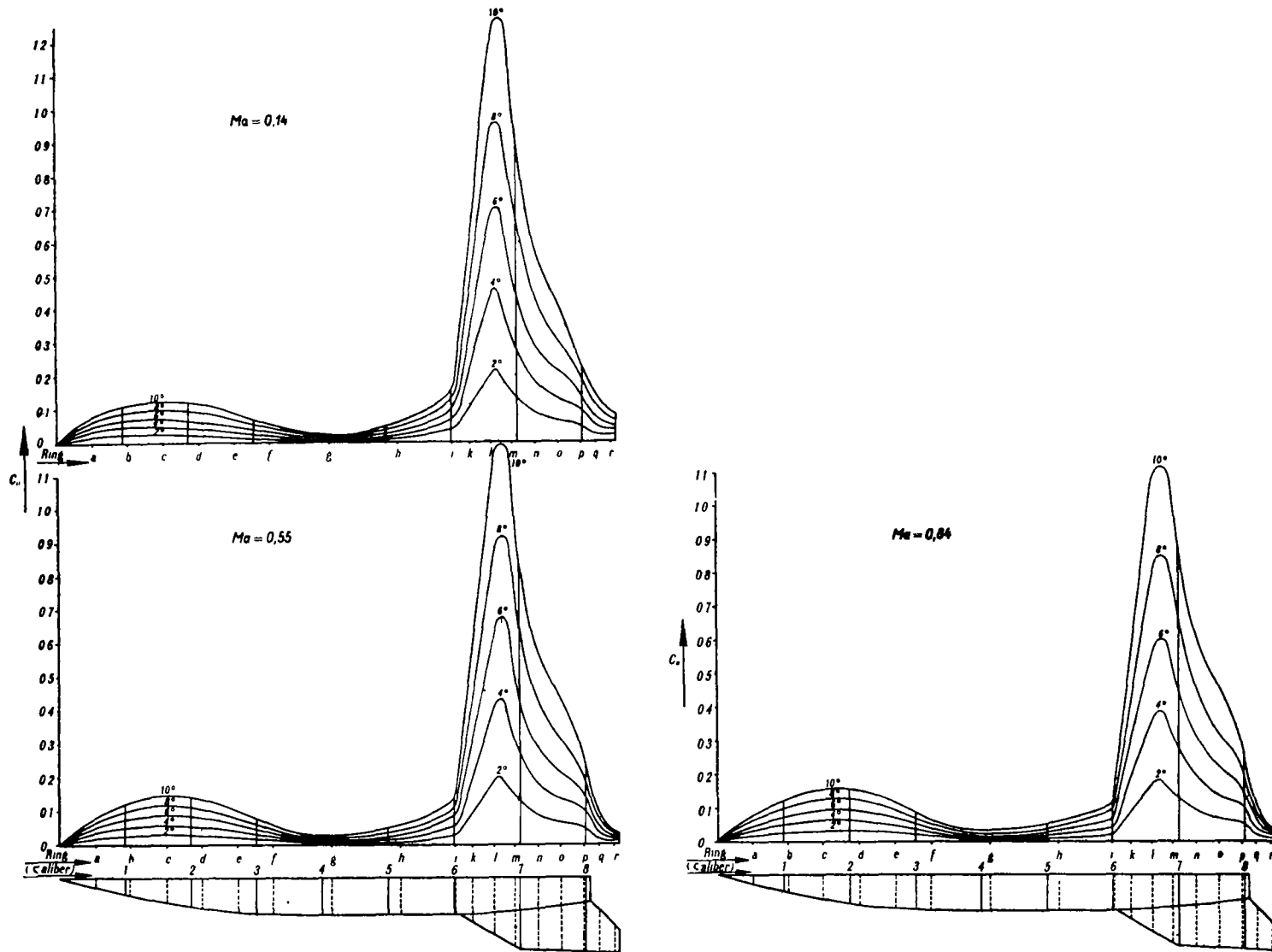


Figure 7.- Pressure distribution test on missile A4VIP, normal force distribution, subsonic speeds.

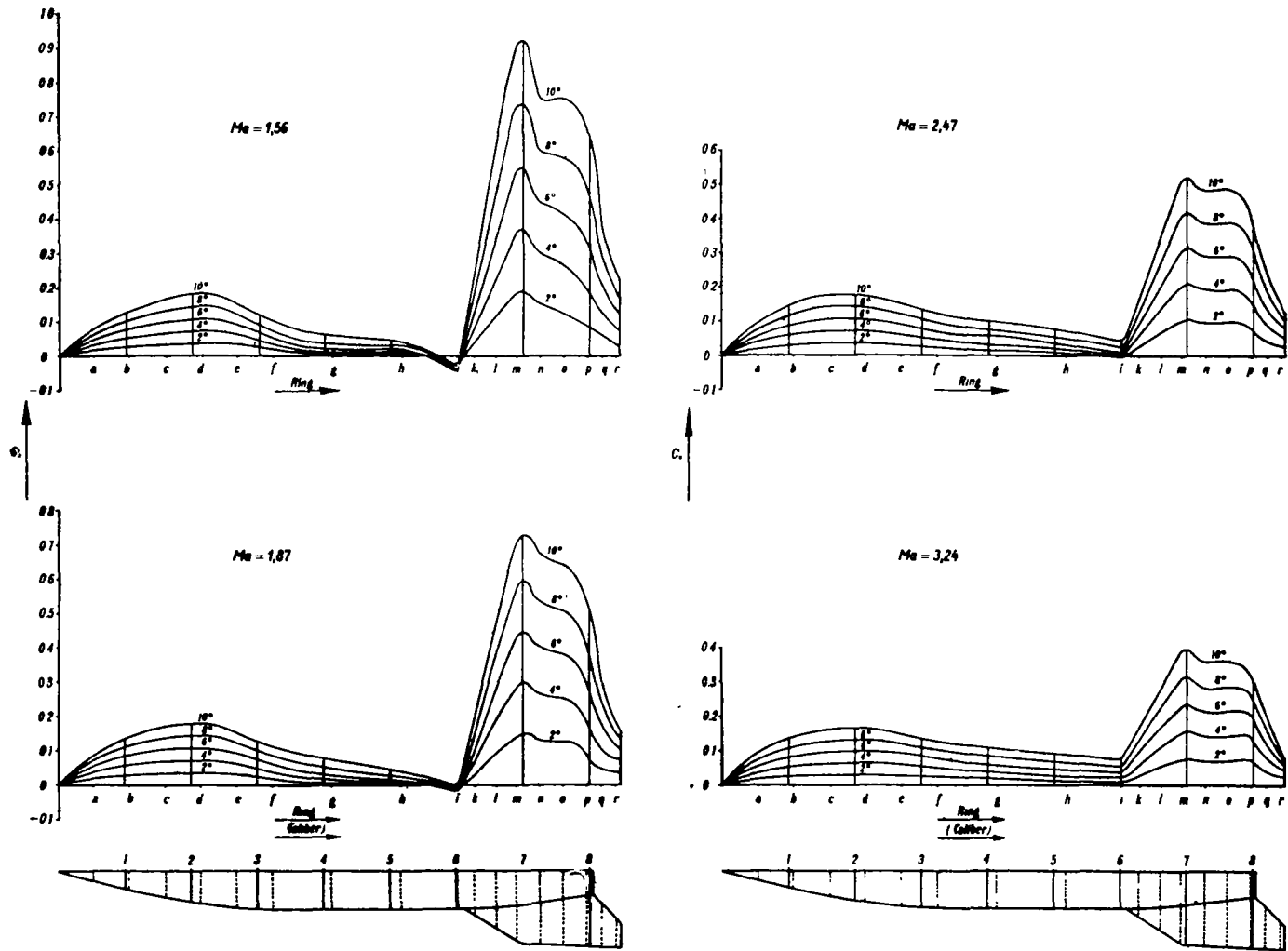


Figure 8.- Pressure distribution test on missile A4VIP, normal force distribution, supersonic speeds.



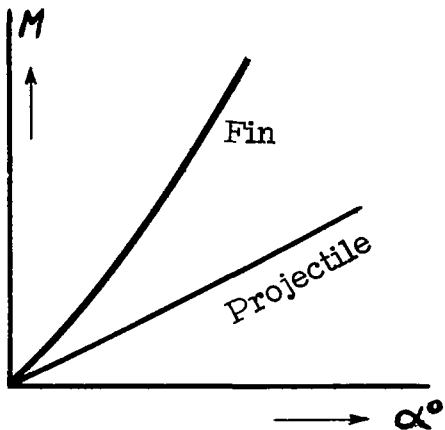


Figure 9.- Moment contribution of fin and nose of a completely stabilized projectile.

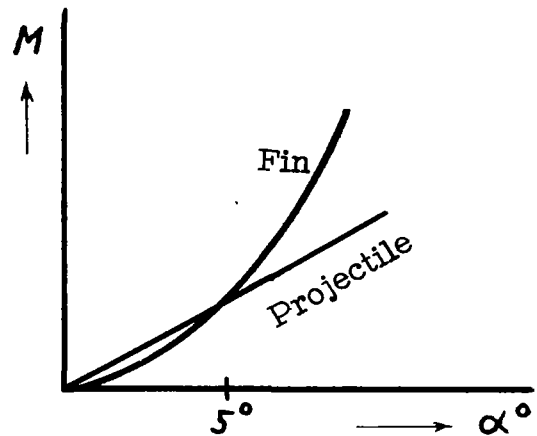


Figure 10.- Moment contribution of fin and nose of an incompletely stabilized projectile.

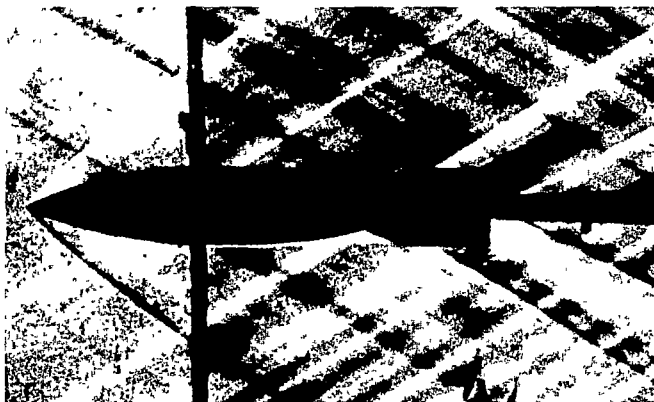


Figure 11.- Separation of flow on a full-caliber projectile in supersonic flow.



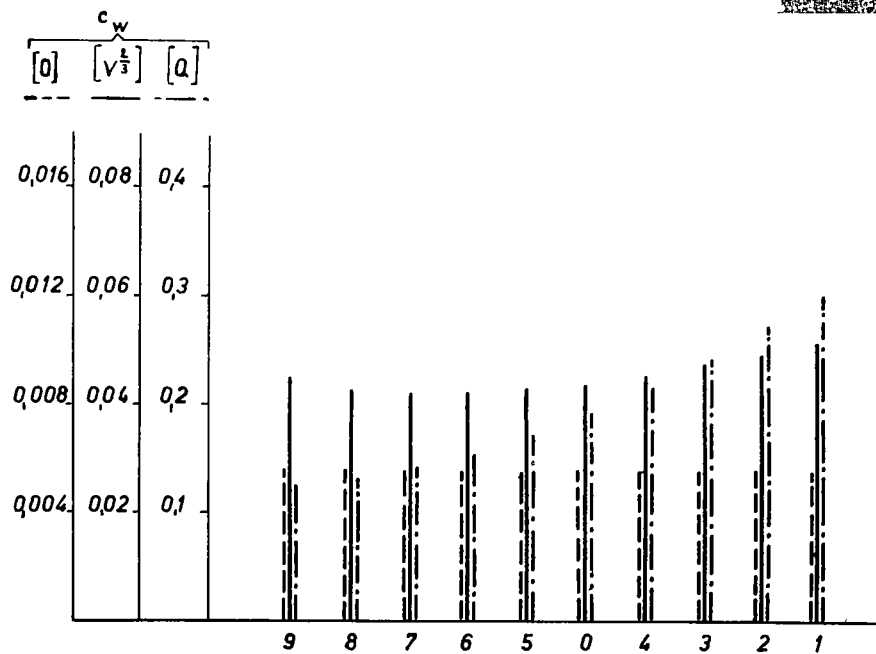
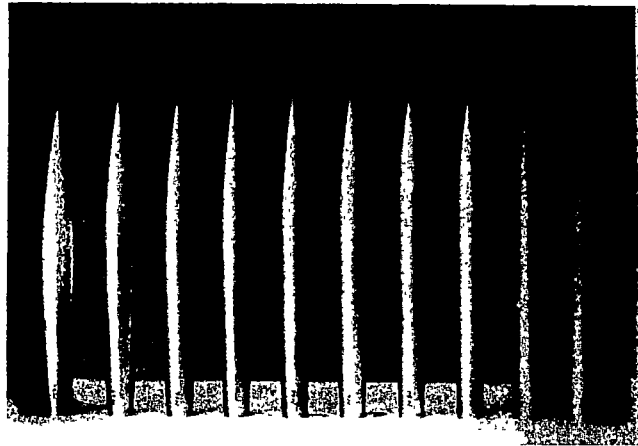


Figure 12.- Body family a.





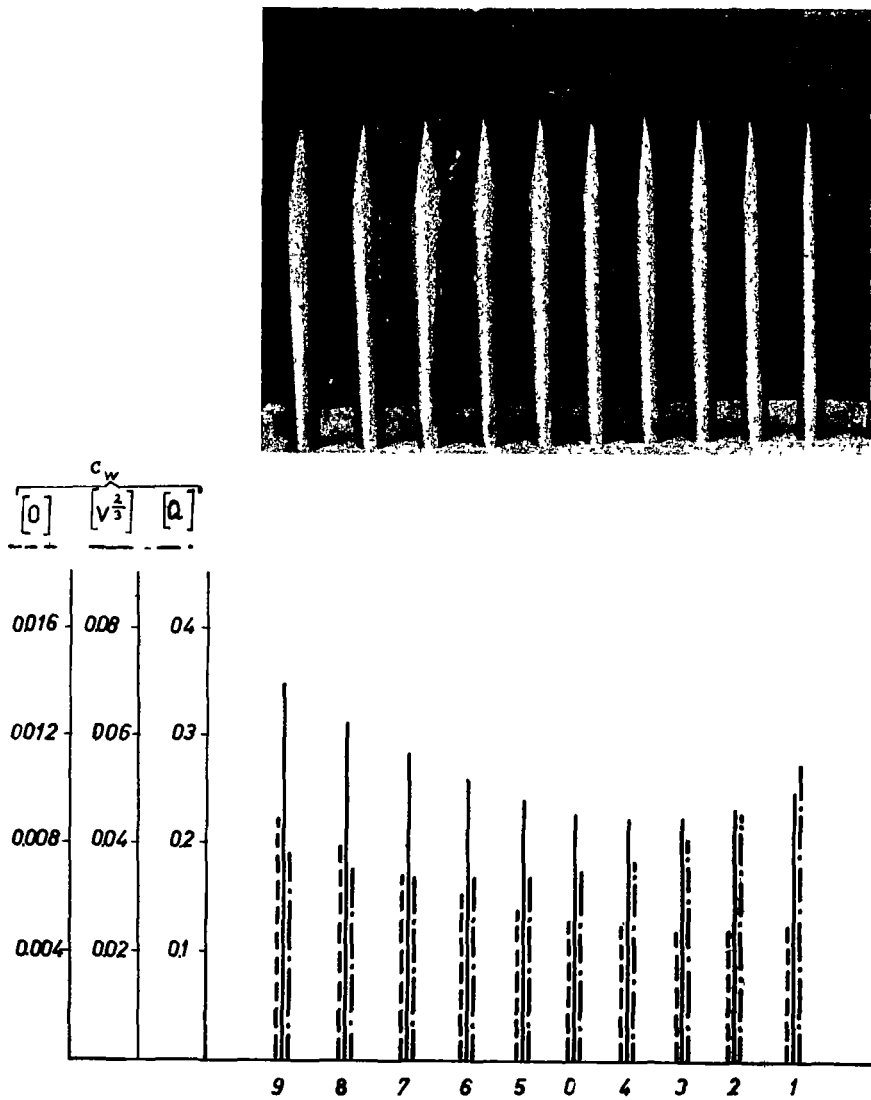


Figure 13.- Body b.



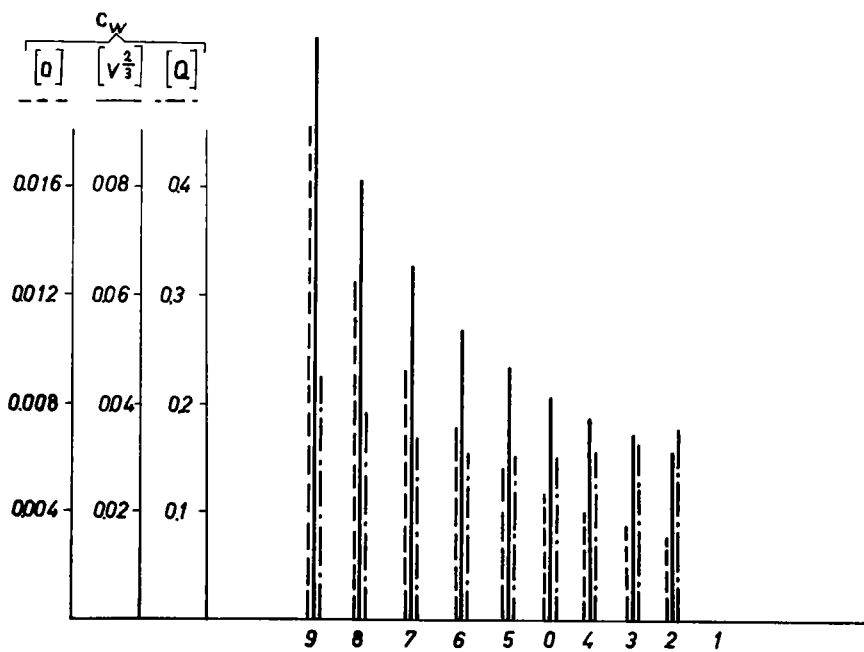
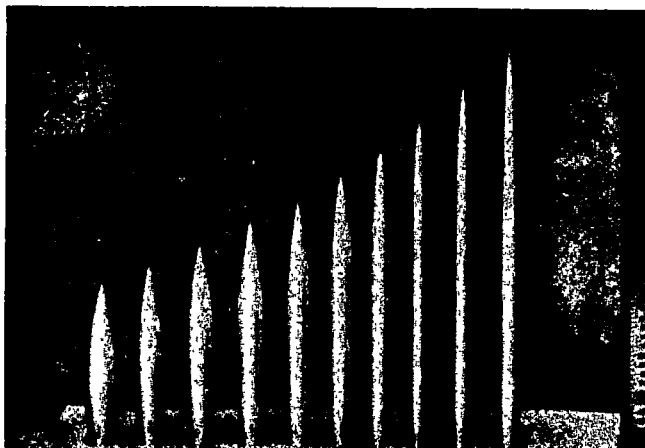


Figure 14.- Body family c.



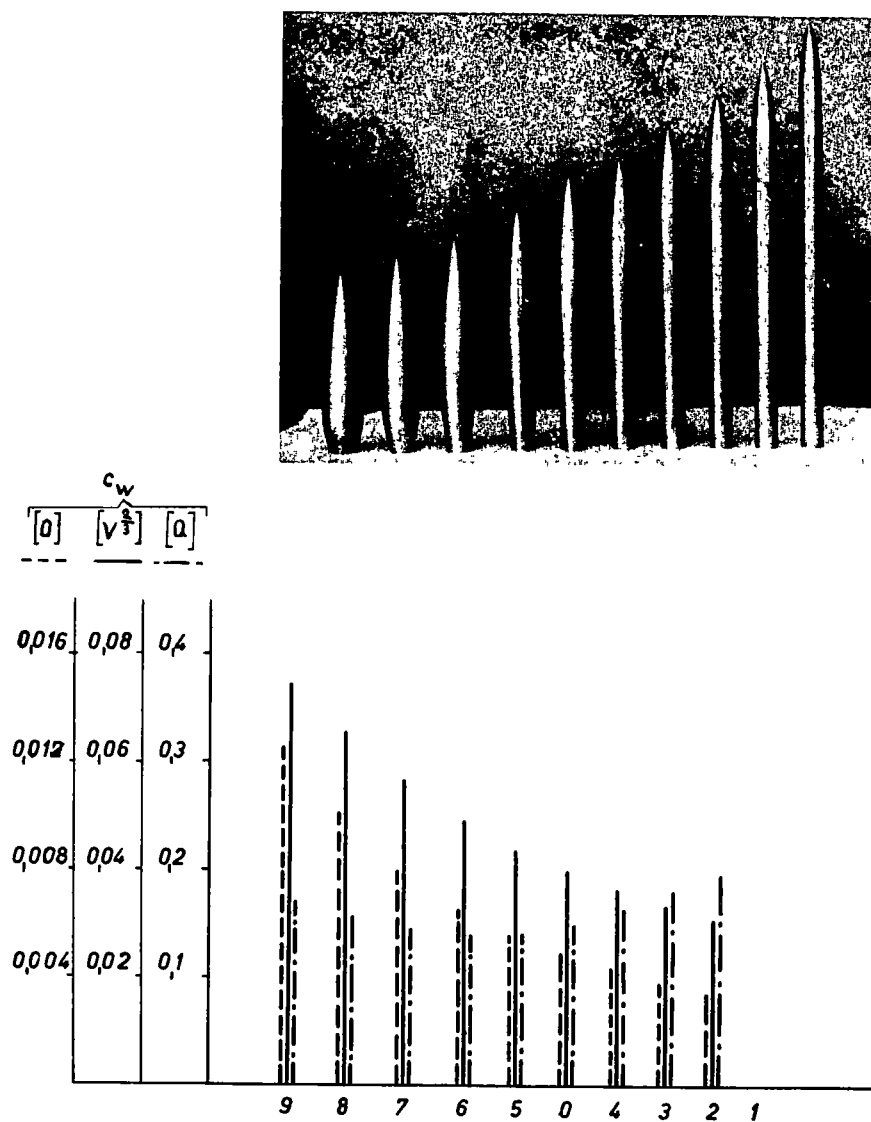


Figure 15.- Body family d.



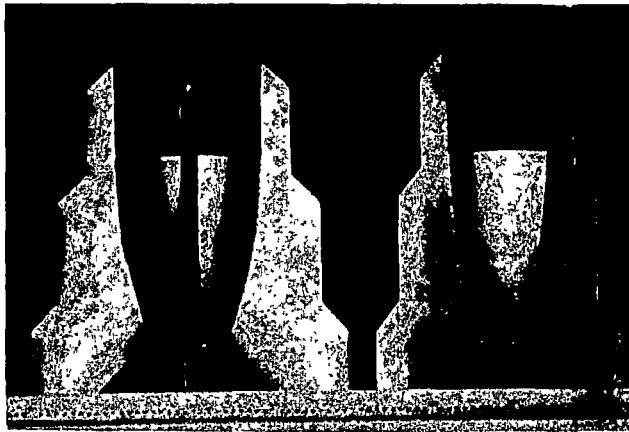


Figure 16.- Three-shoulder fin.

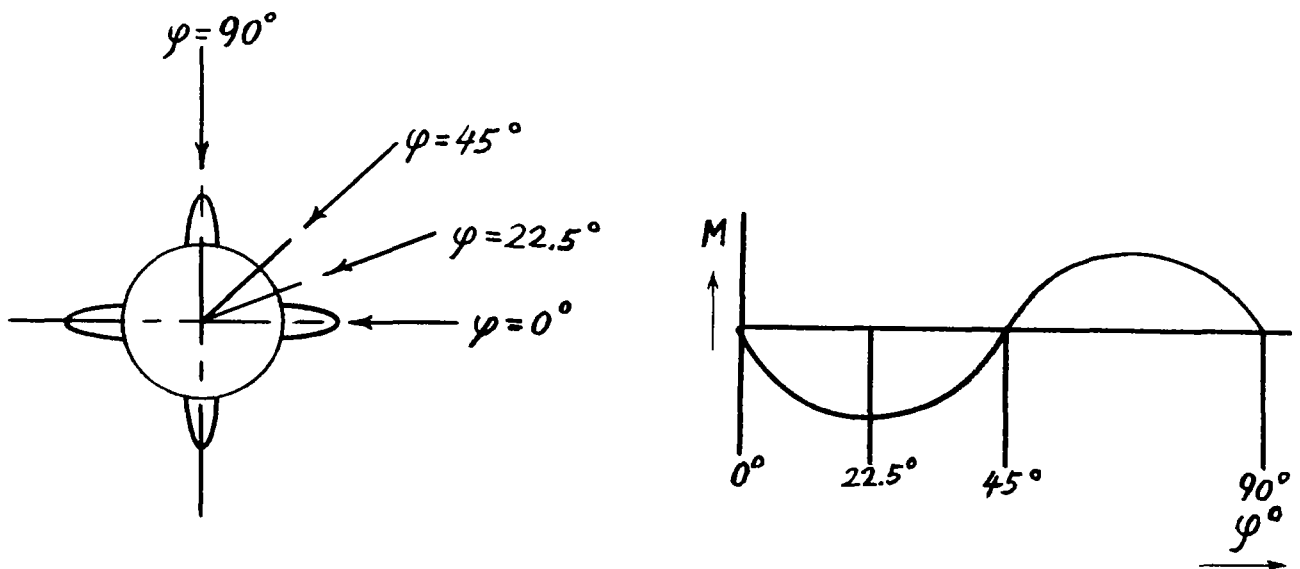


Figure 17.- Rolling moment about longitudinal axis for relative wind at an angle  $\varphi$ .





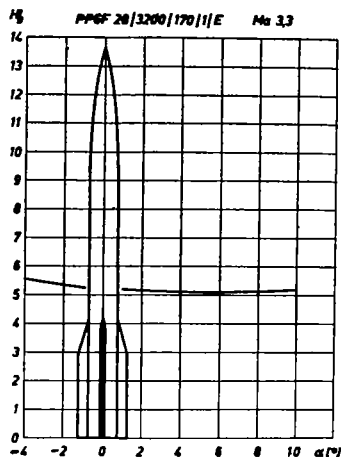


Figure 18.- Point-stable projectile  
c.g. at  $\frac{H}{D} = 6$ .

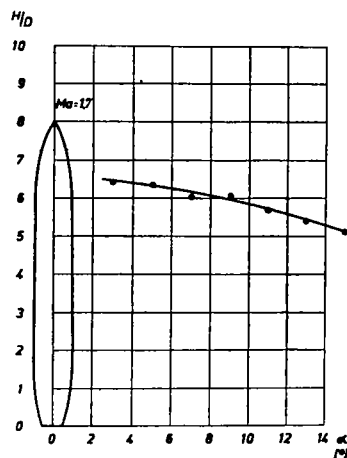


Figure 20.- Unstable projectile c.g. at  
 $\frac{H}{D} = 4$ .

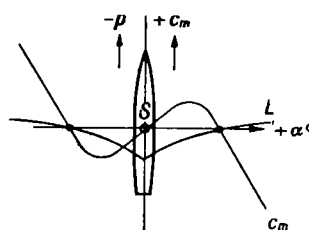
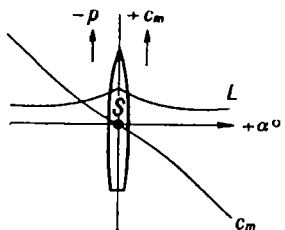
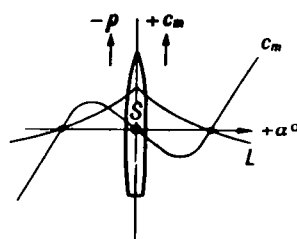
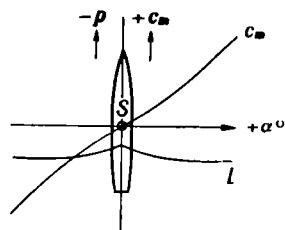


Figure 19.- Stability cases for projectiles.



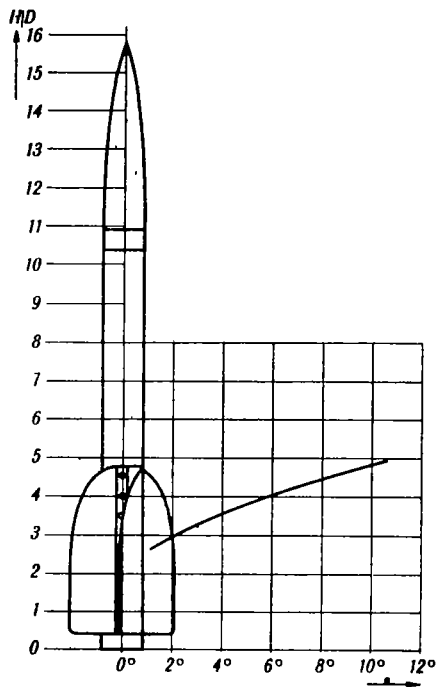


Figure 21.- Projectile with decreasing stability for increasing angles of attack.



Figure 22.- Peenemünde arrow projectile with sliding fins.



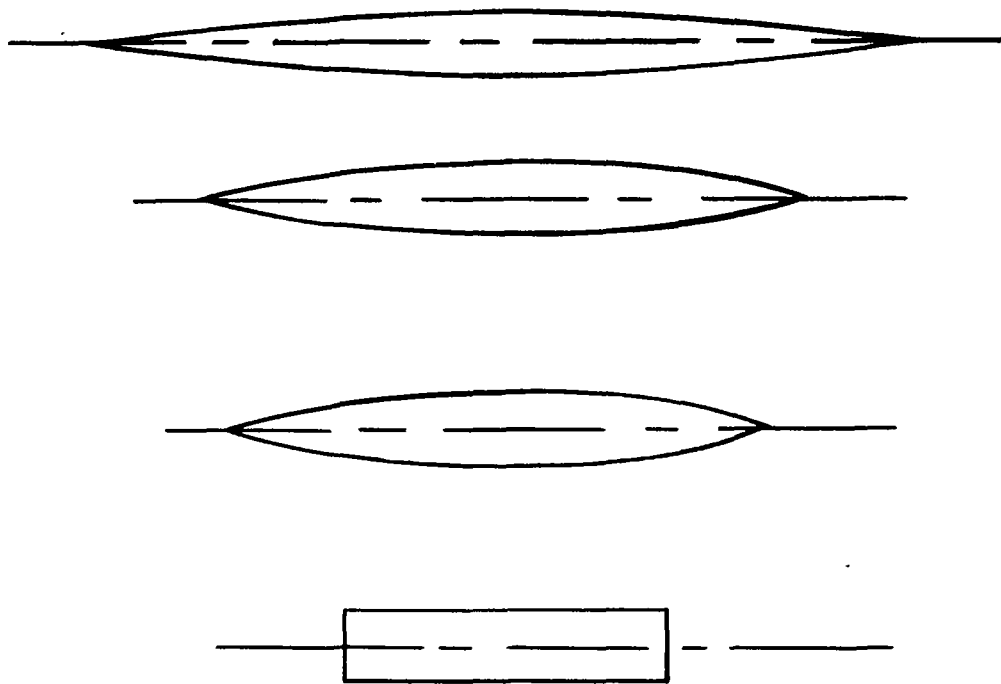


Figure 1.-

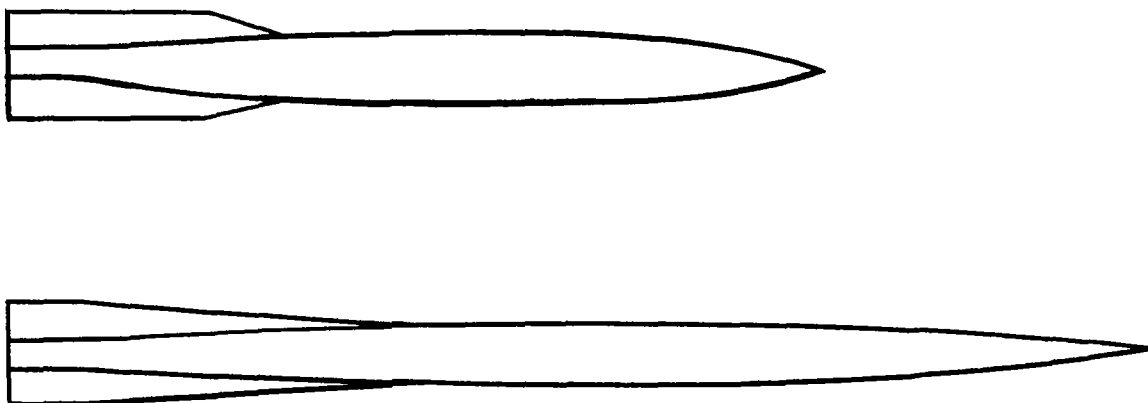


Figure 2.-

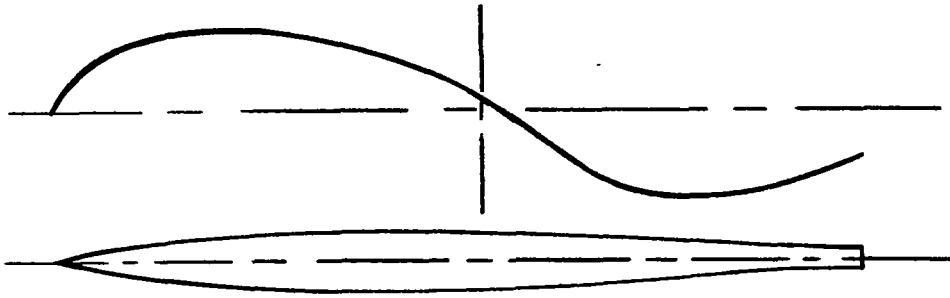


Figure 3.-

$x_0$  range in vacuum at  $v_0 = 3670$  ft/sec.

$x$  range of normal spinning projectile with the same initial velocity.

$x'$  range of arrow projectile (PPE) for  $\frac{D'}{D} = \frac{17}{28} = .61$  and same initial velocity and weight.

Maximum range increase when changing from a full-caliber to a sub-caliber projectile.

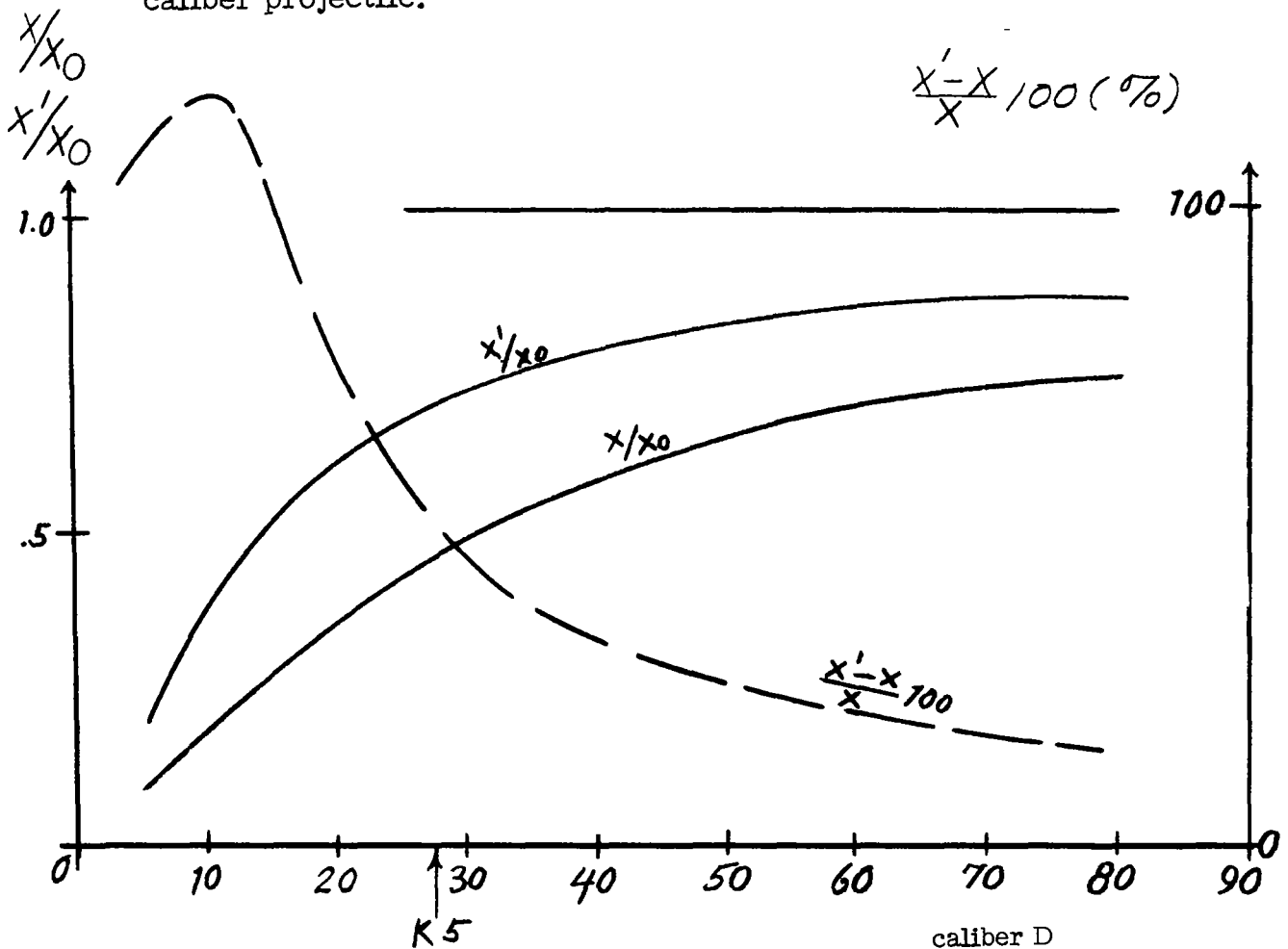


Figure 4.-

NASA Technical Library



3 1176 01441 5765